Due to an error in production, Figs. 3B and 4B were incorrectly positioned in the original version of this paper, which appeared in the December 1987 issue. The correct version of the article is reprinted here in its entirety, and should be used for citational purposes.

DIFFERENTIAL POLARIZATION IMAGING

III. Theory Confirmation. Patterns of Polymerization of Hemoglobin S in Red Blood Sickle Cells

DAVID A. BEACH,* CARLOS BUSTAMANTE,* K. SAM WELLS,* AND KATHRYN M. FOUCAR‡
Department of Chemistry, The University of New Mexico, and ‡The University of New Mexico School of Medicine, Albuquerque, New Mexico 87131

ABSTRACT In this paper we test the predictions of the differential polarization imaging theory developed in the previous two papers. A characterization of the patterns of polymerization of hemoglobin in red blood cells from patients with sickle cell anemia is presented. This system was chosen because it is relatively easy to handle and because previous studies have been done on it.

A differential polarization microscope designed and built in our laboratory was used to carry out this study. This microscope uses an image dissector camera, a photoelastic modulator, and a phase-lock amplifier. This design represents a substantial modification with respect to the instrumentation used in the previous results communicated on this system. Therefore, the results presented here also permit us to confirm the validity of our conclusions.

On the basis of the differential polarization images obtained, models of the patterns of polymerization of the hemoglobin S inside the sickle cells are proposed and their M_{12} and regular images are calculated by the theory. Good agreement between those models and the experimental systems is found, as well as with the results previously reported.

INTRODUCTION

In the two previous papers of this series, we have presented a theory of differential polarization imaging using the Mueller formalism. It has been shown that the polarization-dependent images are true bi-dimensional mappings of the molecular anisotropy of the imaged object. If circular polarizations are used, the chirality of the object is spatially resolved and used at the same time as contrast mechanism to distinguish domains in the object with distinct molecular organization. Similarly, linear polarizations can be used to display the linear dichroism and birefringence of the object.

The first differential polarization images have been recently obtained and communicated by Mickols et al. (1–3). These authors have applied the methodology of differential polarization microscopy to the study of red blood cells from patients with sickle cell anemia. They have shown that the linear dichroism images of these cells, (the M_{12} element of the Mueller matrix) can be used to detect the presence of aligned polymer of hemoglobin S (HbS) inside the red blood cells.

When the blood of patients with sickle cell anemia is placed under hypoxic conditions, the HbS polymerizes and forms oriented bundles inside the red blood cells (4–6). These polymers have been observed under the electron microscope and a number of models have been advanced to explain the way in which the individual hemoglobin molecules pack in the polymer (6–8).

The large absorption coefficient of hemoglobin in the visible spectrum (at the Soret band $\lambda = 435$nm) and the large dichroic signals that they display make these ideal systems to test the predictions of the differential polarization imaging theory developed in the previous two papers.

We have recently built a differential polarization microscope similar to that described previously (2), except that it uses an image dissector camera as an imaging device, and a photoelastic modulator to generate the orthogonal polarizations of the light. A detailed description of this instrument will be published in another journal (Beach, D. A., K. S. Wells, C. Bustamante, and F. K. Husher, manuscript submitted for publication). In this paper, we present the results of a study, also on sickled red blood cells, using this newly built instrument. These images show how the results obtained in the previous two papers can be used to deduce the modes of alignment of the HbS polymers inside the red blood cells. The theory of differential polarization imaging is used to compute the images predicted from these models.

A comparison of our results with those obtained previously (1) is of interest, since these two sets of studies have been carried out with instrumentation that differs substantially in the signal generation. Our results point out the enormous potential of this newly developed technique as a

specific and sensitive probe of the molecular organization of biological samples.

MATERIALS AND METHODS

Sample Preparation

Heparinized blood from a sickle cell anemia patient was obtained. The hematocrit of the sample was then measured. Hematocrit values between 22 and 30% were obtained in the cases studied. The blood was centrifuged for 5 min at 3,000 rpm to separate the cellular elements from the plasma, which was discarded. The cells were resuspended gently in a variable amount of 50 mM buffer phosphate, 150 mM NaCl, pH 7.4, to maintain the hematocrit at 20%. The resuspended cells were centrifuged again at 3,000 rpm. This process was repeated four times to remove all the plasma proteins. In the last resuspension the hematocrit was reduced to 10%.

To induce sickling, the blood was deoxygenated by equilibration in a 100% N_2 atmosphere for 2 h. This process was carried out in a specially designed two-entrance tube. The hypoxic cells were then fixed with an equal volume of 3% glutaraldehyde/50 mM phosphate buffer. For the final preparation, the fixed samples were diluted in saline buffer to a hematocrit of ~0.5%. A 20-μl drop of blood was placed between two strain-free quartz coverslips, which were sealed to prevent dehydration of the cells.

Differential Polarization Microscope

A differential polarization microscope that uses an image dissector tube as the imaging device has been built in our laboratory (see Fig. 1). The incident light from a monochromatic source is passed through a large aperture Glan-Thompson polarizer and enters a photoelastic polarization modulator. Here, the polarization of the incident light is modulated between orthogonal linear polarizations. The modulated light is then focused onto the specimen placed in a strain-free optics Universal Zeiss microscope. The image is projected onto the photocathode surface of the image dissector tube camera. The image dissector camera outputs an analog voltage proportional to the light intensity at each pixel location in the image. The output signal of the camera is then passed simultaneously to a lock-in amplifier and an analog integrator. The lock-in amplifier measures that part of the signal that is proportional to the difference in intensity transmitted by the object for the two incident polarizations. The integrator measures the average transmitted light intensity through the specimen.

The image dissector camera scans the image, sitting at each pixel location for a programmable period of time. The voltage outputs from both the lock-in amplifier and the integrator are averaged for the dwell time at each pixel and digitized to 12-bit resolution by a computer for each location in the image. The digitized images from the lock-in amplifier and integrator are stored as separate data files labeled "difference" and "total," respectively. The difference file is divided by the total file to produce a third normalized image that is proportional to the M_{12} or linear dichroism image. The images generated are then displayed on a video monitor for visualization. The images generated range in spatial resolution from 32 × 32 up to 512 × 512 pixels.

All the images to be presented in the next section were obtained using a Zeiss ultra-fluar strain-free, 100× objective. The wavelength of the incident light was 435 nm.

RESULTS

Deoxygenated red blood cells containing HbS develop a wide variety of morphological abnormalities. This is thought to be a direct result of the formation of HbS polymer inside the cell. This process is accompanied by the formation of bundles of hemoglobin polymers inside the red cell. It has been known for some time that these

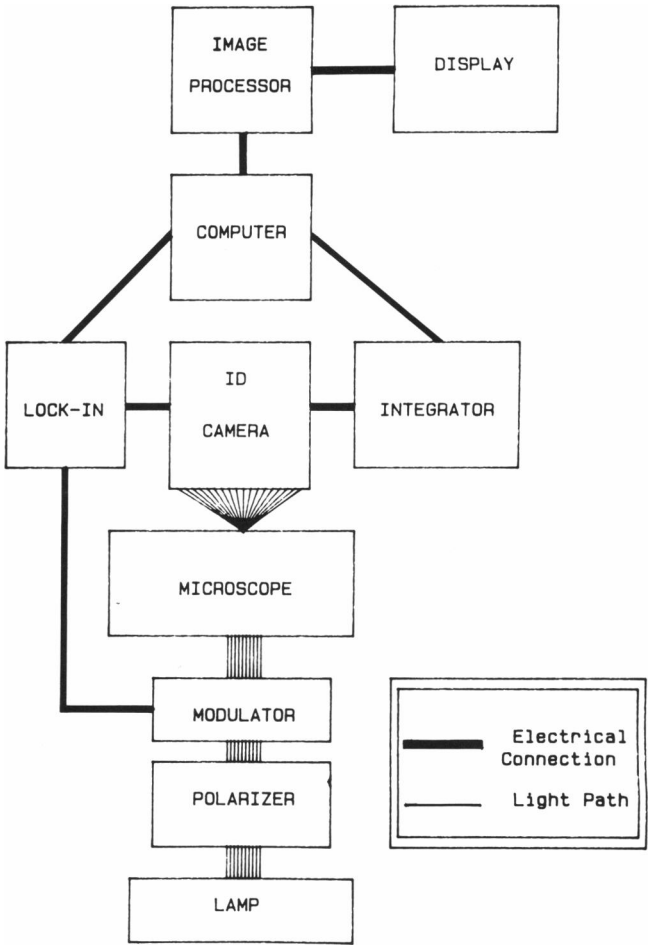

FIGURE 1 Block diagram of the differential polarization microscope. Light from a Xenon arc lamp is passed through an interference filter to a polarizer and a modulator. The modulated polarizations of light are incident upon the sample placed in the microscope. The image of the sample is projected on an Image dissector camera. The signal from the camera is passed both to a lock-in amplifier, which measures the difference due to the orthogonal polarizations of light, and an integrator which measures the average transmitted intensity. The signals are digitized and stored in a computer.

domains of aligned HbS molecules in the cells display distinctive optical properties such as linear dichroism and linear birefringence (1, 5, 10–12). The orientation of the heme groups was determined by Perutz and Mitchison (9), and later by Hofrichter (5), to be approximately perpendicular to the polymer axis. Furthermore, the basic structure of the polymers is known from light scattering studies (13), electron microscopy (6–8, 14), and x-ray diffraction studies (15). Mickols et al. (1, 3) have shown that this system is particularly useful for evaluating the performance of the differential polarization method, because hemoglobin has strong extinction coefficients in the Soret band (406–435 nm), and sickled red blood cells display dichroic signals of the order of a few parts per 100. Since this system has been so well characterized, it is ideal to test the theory presented in the previous papers of this series.

The linear dichroism images presented confirmed earlier

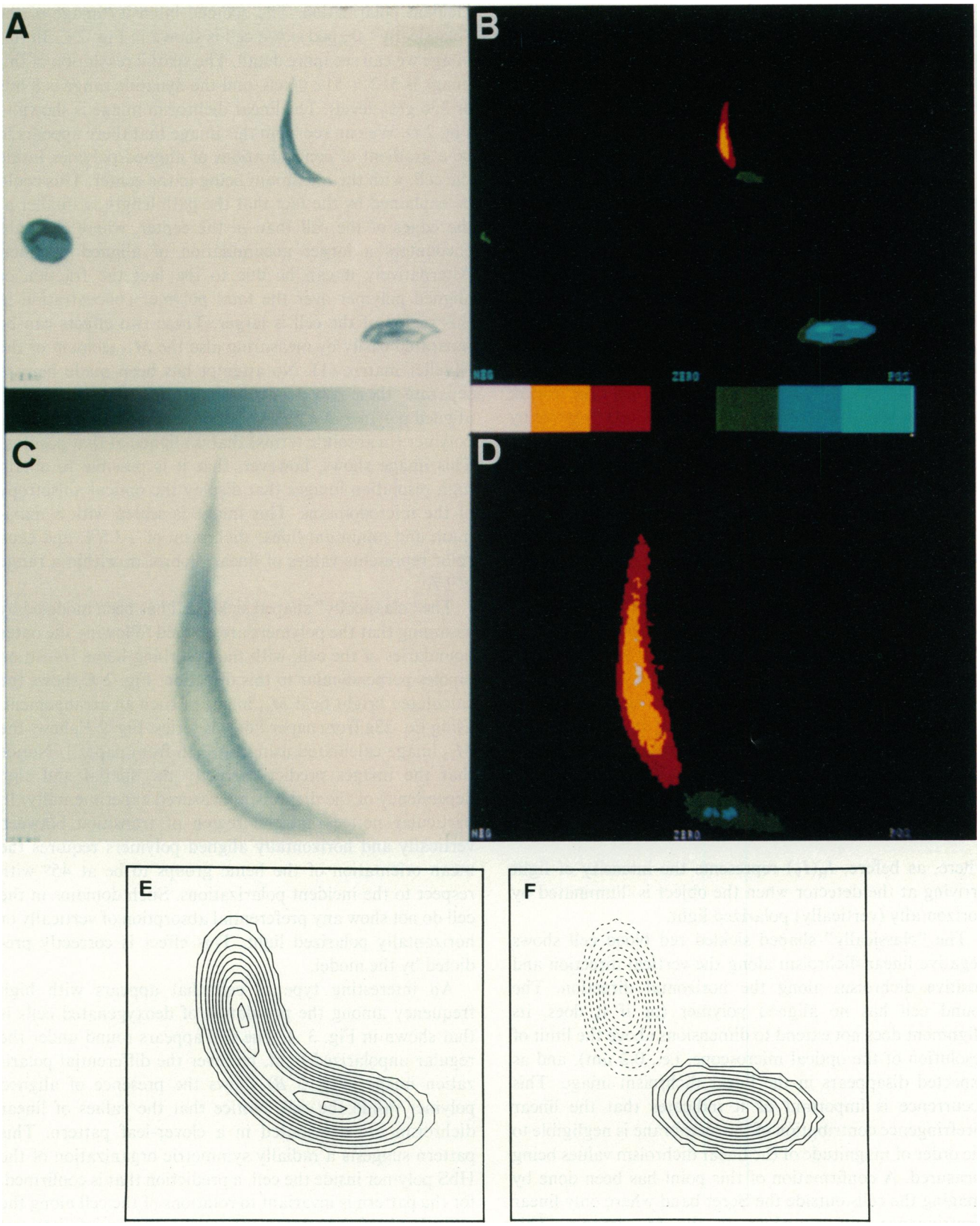

FIGURE 2 Images of red blood cells from a patient with sickle cell anemia. The intensity images are shown, in gray-scale; and the differential images in pseudo-color. The magnification is 1,600. The color code is shown at the bottom of the images. The cells were imaged with 435- nm − + 10-nm light. The linear dichroism ranges from +0.03 to −0.03. The image is 340 pixels on a side. (*A*) Intensity image of three blood cells. (*B*) Differential image of the same three cells. (*C*) Zoomed intensity image of the sickle cell in *a*. (*D*) Differential image of the same cell in *c*. (*E*) Calculated intensity image of sickle cell. (*F*) Calculated differential image of sickle cell; the solid lines represent positive dichroism and the dashed lines negative.

results (1) that show that differential polarization imaging can be used to map the polymer organization inside the cell. Simple uniaxial models of the distribution of alignment and orientation of the hemoglobin are then used to obtain theoretical linear dichroism images to show the agreement of the experimental results with the calculations.

It is possible to present the digitized images in a variety of ways. In this paper we will present the intensity (total) images in normal black-and-white or gray scale, and the linear dichroism images in pseudo-color. The optical configuration of the polarizer and photoelastic modulator was chosen as "horizontal" (along the color bars below the image) and "vertical" perpendicular to the previous one. To simplify the interpretation of the differential polarization images we have used only seven colors. These colors represent the magnitude and sign of the linear dichroism; maximum negative is represented by pink, less negative by yellow, and slightly negative by red. Zero or no linear dichroism is represented by black, slightly positive is green, larger positive by dark blue, and maximum positive linear dichroism is represented by light blue.

Fig. 2 *A* is an image of the microscope field showing three cells with different morphologies. The top cell has a "classical" sickle shape, the round cell to the lower left is a normal cell, and the cell to the lower right is a sickle cell with a "yam" shape. This is the total image representing the average transmitted intensity from the two orthogonal linear polarizations incident on the sample, i.e., the image obtained with regular unpolarized light. The image in Fig. 2 *B* is the pseudo-color representation of the linear dichroism of the cells. The linear dichroism image is defined here as in the previous papers of this series, that is

$$(I_H - I_V)/(I_H + I_V),$$

where, as before, $I_H(I_V)$ represents the intensity of light arriving at the detector when the object is illuminated by horizontally (vertically) polarized light.

The "classically" shaped sickled red blood cell shows negative linear dichroism along the vertical direction and positive dichroism along the horizontal direction. The round cell has no aligned polymer (or if it does, its alignment does not extend to dimensions above the limit of resolution of the optical microscope, i.e., 0.2 μm), and as expected disappears in the linear dichroism image. This occurrence is important as it indicates that the linear birefringence contribution of the membrane is negligible to the order of magnitude of the linear dichroism values being measured. A confirmation of this point has been done by imaging the cells outside the Soret band where only linear birefringence can contribute to the M_{12} images. This contribution was found to be an order of magnitude smaller than the dichroism values. The "yam" cell because of the positive values (green, blue, and light blue colors) shows all of the HbS polymer to be oriented horizontal to the incident polarization. The zoomed intensity image of the "classically" shaped sickle cell is shown in Fig. 2 *C*. In this image we can see more detail. The spatial resolution of this image is 512 × 512 pixels, and the dynamic range is 8 bits or 256 gray levels. The linear dichroism image is shown in Fig. 2 *D*. We can see from this image that there appears to be a gradient of concentrations of aligned polymer inside the cell, with the maximum being in the center. This could be explained by the fact that the path length is smaller at the edges of the cell than in the center, where the light encounters a larger accumulation of aligned polymer. Alternatively it can be due to the fact the fraction of aligned polymer over the total polymer concentration in this region of the cell is larger. These two effects can be separated easily by measuring also the M_{13} element of the Mueller matrix (1). No attempt has been made here to separate these two contributions, i.e., the fraction of aligned polymer at a given position and the total amount of polymer (in absolute terms) that is aligned at that position. This image shows, however, that it is possible to obtain high resolution images that display the optical anisotropy of the microdomains. This image is scaled with a maximum and minimum linear dichroism of ±3.5%, and each color represents values of linear dichroism within a range of 1%.

The "classically" shaped sickle cell has been modeled by assuming that the polymers are aligned following the outer boundaries of the cell, with the absorbing heme transition dipoles perpendicular to this direction. Fig. 2 *E* shows the calculated bright field M_{11} image of such an arrangement, using Eq. 23a from paper I of this series. Fig. 2 *F* shows the M_{12} image calculated using Eq. 23b from paper I. Notice that the images predict correctly the spatial and sign dependency of the dichroism measured experimentally. In particular notice that the region of transition between vertically and horizontally aligned polymers requires the mean orientation of the heme groups to be at 45° with respect to the incident polarizations. Such domains in the cell do not show any preferential absorption of vertically or horizontally polarized light. This effect is correctly predicted by the model.

An interesting type of cell that appears with high frequency among the population of deoxygenated cells is that shown in Fig. 3 *A*. The cell appears round under the regular unpolarized light, however the differential polarization image (Fig. 3 *B*) shows the presence of aligned polymer inside the cell. Notice that the values of linear dichroism are distributed in a clover-leaf pattern. This pattern suggests a radially symmetric organization of the HbS polymer inside the cell, a prediction that is confirmed, for the pattern is invariant to rotations of the cell along the optical axis of the microscope (see section on infinitesimal rotations in paper II of this series). We propose that the hemoglobin in this case is distributed in a fan-like fashion, with the polymer following a radial distribution. This model is particularly suggestive for it could indicate a

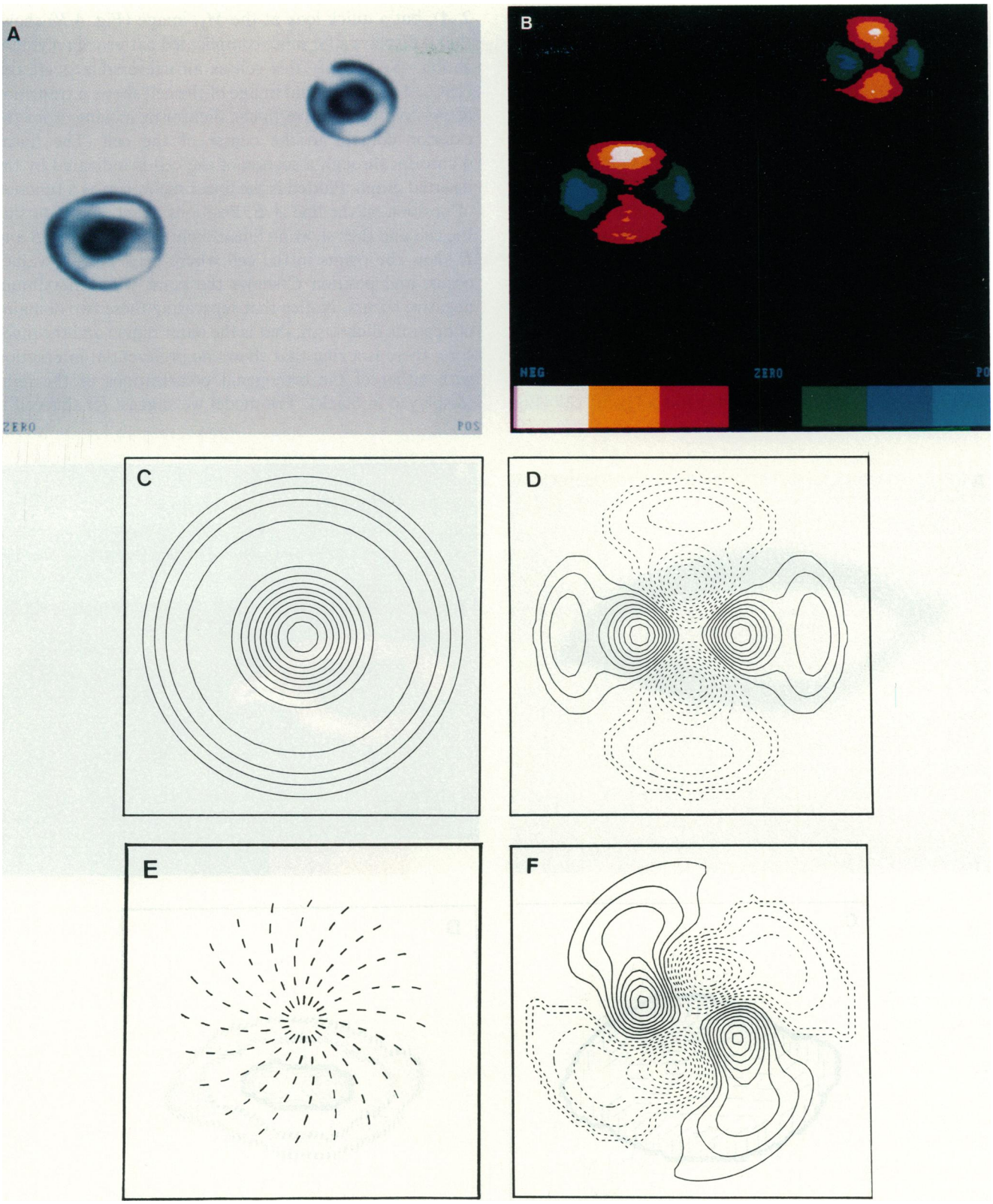

FIGURE 3 Images of cells which appear to be normal red blood cells. Magnification, 1,600. (*A*) Intensity image of two round red blood cells. (*B*) Differential image of the same cells. (*C*) Calculated image of a round cell with the polymer alignment distributed in a radial fashion. (*D*) Calculated differential image of the modeled cell; solid lines represent positive values and dashed lines represent negative values. (*E*) Model of the radial polymers twisted in a clockwise direction. (*F*) Calculated differential image of the model.

mechanism of nucleation of the polymerization process in the membrane, as has been proposed in the literature (16, 17). Fig. 3, *C* and *D* shows the regular and differential polarization images, respectively, calculated with the theory. Notice that this model predicts correctly the pattern observed experimentally. In a few instances we have observed similar clover leaf patterns (not presented here) in which the lobes are not aligned in a cross fashion as they appear above, but the lobes appear rotated clockwise between 40° and 45° with respect to the laboratory frames. Fig. 3, *E* and *F* shows that such spatial distribution of the linear dichroism signals can be accounted for by a radial model in which the polymers swirl in the counterclockwise sense as they radiate from the center towards the outer borders of the cell.

Fig. 4 *A* shows an image of a particularly interesting cell. This cell looks morphologically like a "yam" cell (Fig. 2 *A*), but a quick look at the M_{12} image (Fig. 4 *B*) shows that it displays a far more complicated pattern of polymerization. We identify this cell as an irreversible sickle cell (ISC). The differential image of the cell shows a transition of positive to negative linear dichroism moving from the exterior domain to the center of the cell. The linear dichroism through a section of the cell is indicated by the inserted graph. Plotted is the linear dichroism as a function of position on the line *A-E*. Positions *A* and *E* are outside the cell and thus show no linear dichroism. Positions *B* and *D* show the points in the cell where peak positive values occur, and position *C* shows the point where maximum negative occurs. Notice that separating these two domains of opposite dichroism, that is the outer region and the inner core, there is a ring that shows no preferential interaction with either of the orthogonal polarizations of the light (displayed in black). The model we suggest for this cell is

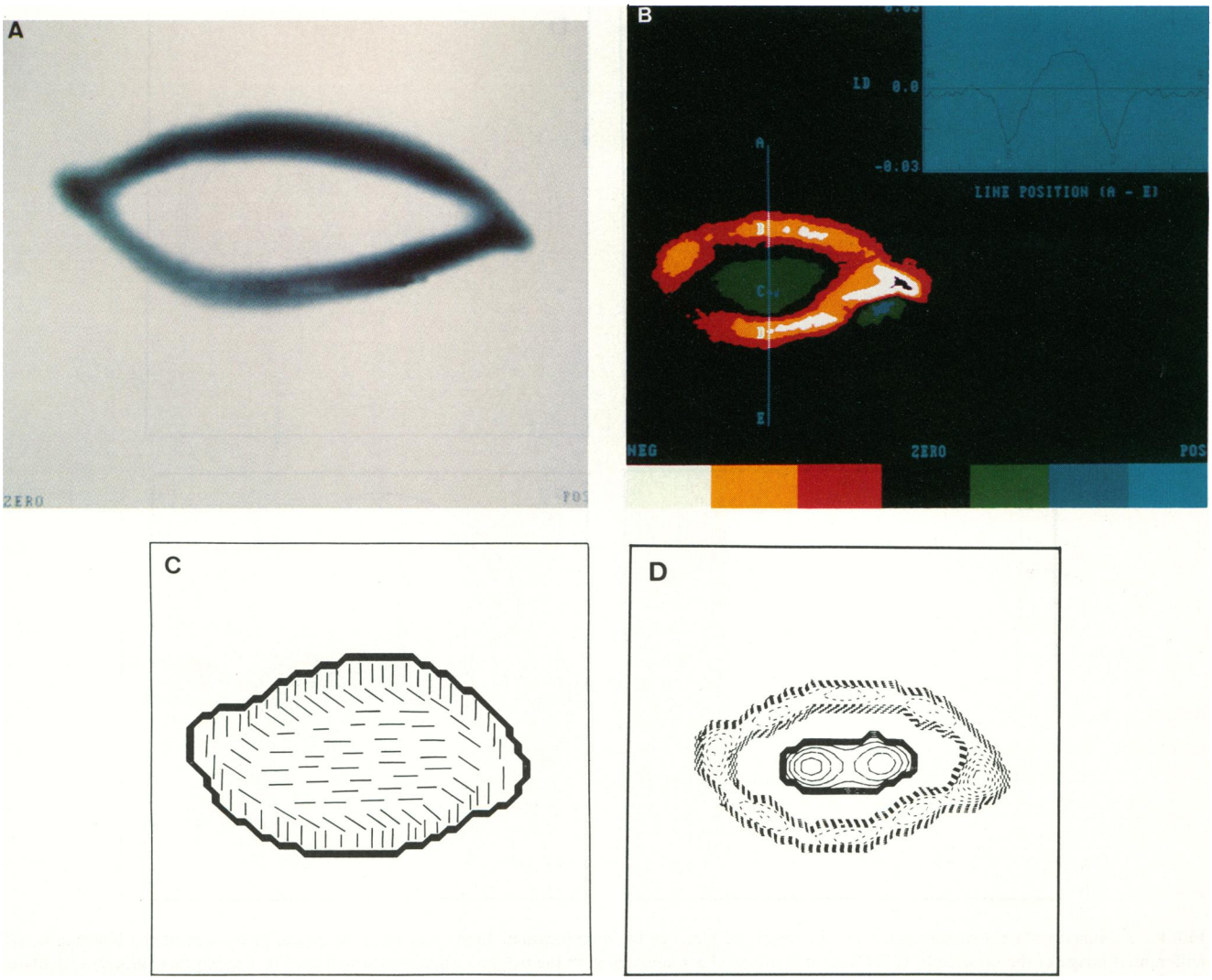

FIGURE 4 Images of an irreversible sickle cell (ISC). Magnification, 1,600. (*A*) Intensity image of the cell, (*B*) measured differential image of the cell, (*C*) model of the cell showing the proposed polymer alignment within the cell, (*D*) calculated image of the cell; solid lines represent positive values and dashed lines represent negative values.

depicted in Fig. 4 *C* in which the hemoglobin polymer is aligned in a sigmoidal fashion throughout the cell. Fig. 4 *D* shows the pattern predicted by the theory. This type of cell is particularly common in oxygenated sickle cell blood samples, and we have observed it a few times in the deoxygenated state. It is interesting to note that the shape of this cell does not vary substantially from the oxygenated to the deoxygenated state; however, no substantial amount of polymer seems to be present in the oxygenated case (results not shown). Notice also that the alignment of the polymers in this case is perpendicular to the cell surface, as in the case of the clover-leaf cells of Fig. 3.

DISCUSSION

The predictions of the theory derived in the previous two papers of this series have been tested by matching the experimental results to theoretical calculations on various patterns of polymerization. In all the cases analyzed we have found that our results agree by and large with the results obtained previously, using a completely different microscope design and imaging device (1–3). This agreement is important for it points out the feasibility of the differential polarization imaging studies and the enormous potential of differential polarization imaging as a method of structural analysis. The qualitative agreement of the calculations with the experimental results is excellent in the system chosen, but quantitative agreement will require substantial improvements in the complexity of the models tested.

The systems presented in this paper are characterized by relatively simple patterns of polymerization of the hemoglobin inside the red blood cells, and thus they are an ideal system to test the predictions of the theory. Furthermore, these systems have been analyzed and characterized by other methodologies, substantially simplifying the comparison with our results.

Since 1940, when Sherman (19) showed that sickled cells were birefringent, optical polarization methods have been used to characterize their morphology and hemoglobin polymer formation. Perutz and Mitchison in 1950 (9) used polarized microscopy to study the structure of sickled cells. Sickled cells that were straight and tubular, when observed between crossed polarizers, lit up with a deep blue color, and extinguished with a 90° rotation. They concluded that sickled cells exhibit both linear birefringence and linear dichroism and that the heme groups of the polymerized hemoglobin were oriented perpendicular to the polymer axis. A study by Hofrichter et al. (5) in 1973 provides more recent evidence for the orientation of the heme groups in the hemoglobin polymer. These authors used polarization absorption microscopy to obtain quantitative data on the possible orientation of the HbS molecules in sickle-cell fibers. They measured the polarization ratio ($P = A_\perp/A_\parallel$) in 1-μm^2 sections of single sickle cells. Where $A_\perp$ ($A_\parallel$) is the absorption of incident light by the hemoglobin polymer, which is polarized perpendicular (parallel) to the heme groups. They found that the highest polarization ratio in these sections was $P = 3.0$, and confirmed that the heme groups were oriented, forming an angle between 17° and 20° with respect to the direction perpendicular to the polymer axis.

It has been established that the transitions responsible for the absorption of hemoglobin at the Soret band are all *x-y* polarized, i.e., lying in the plane of the heme group (17, 18). Indeed, bands whose transitions dipole moments are directed perpendicular to the plane of the heme group are much weaker than the in-plane transitions that give rise to the Soret band. Furthermore, the out-of-plane transitions are centered below 310 nm (17, 18). Thus, the contribution of these *z*-polarized transitions can be completely neglected in analyzing the data obtained at the visible wavelengths. From the sign and magnitude of the differential polarization signal at every position, it is straightforward to determine the orientation of the heme groups in the polymerized hemoglobin at those same positions. The sign of the difference depicted in the images, that is

$$(I_H - I_V)/(I_H + I_V),$$

will be positive if the heme groups are aligned preferentially along the vertical axis in the laboratory frame of reference, and negative if the heme groups are preferentially aligned along the horizontal laboratory coordinate. This information is therefore enough to map the direction of alignment of the polymer inside the red blood sickle cells. This information was used to build the models presented here.

The results of Hofrichter et al. (5) have been used by Mickols et al. (1) to show how the differential polarization microscope could be used to quantify the amount and direction of oriented hemoglobin polymer in sickled red blood cells. They showed that the photon extinction cross-sections per hemoglobin molecule could be calculated, from which the amount and distribution of oriented hemoglobin molecules per μm^2 can be obtained. The extended sensitivity, attained by subtracting out everything in the image that is the same in the interaction with the two opposite polarizations, is what gives the differential polarization imaging its advantage over the other polarization methodologies.

Evidence that supports the pattern of polymerization that we have suggested here for the sickled cells shown in Fig. 3 *B* has been given by White (6). Photographs of squashed sickle cells under phase-contrast microscopy showed the hemoglobin polymer to be distributed in a "fan-like" pattern. Also, similar radial configurations resulted when diluted solutions of HbS were subjected to conditions leading to the formation of hemoglobin gels in vitro.

The differential polarization microscope would be well suited for studies on the effect of the cell membrane in the

polymerization process. There is still much speculation about the role of the cell membrane in the formation of polymer in cells of patients with sickle cell anemia, particularly when these are exposed to hypoxic conditions. Some researchers have concluded that there is not much evidence that the membrane plays any role at all. A study of the effect of cell membrane preparations on polymerization of sickle hemoglobin, by Goldberg et al. (16), did not show any evidence for facilitation of sickling by nucleation sites on the cell membrane. In a more recent experiment Mizukami et al. (11) have studied the effect of the cell membranes on the rate of polymer formation in *in vitro* solutions of HbS. They concluded that the inner surface of the membranes could behave as a template for polymer formation at high rates of deoxygenation. Through a polarizing microscope, they measured the birefringence of a thin layer solution of HbS while exposing it to cell membranes prepared in various ways. The microscope served only to collect the transmitted light from the sample, and not as an imaging device. Thus, the birefringence measured represented an average throughout the field of view. With the differential polarization microscope, similar experiments are possible. Imaging a single cell as a function of the degree of deoxygenation may permit the visualization of the effects the membrane has on the polymerization process. These studies are currently in progress in our laboratory.

Differential polarization imaging is beginning to show its usefulness in the study of biological systems. This technique is simply an extension of proven optical polarization methods (e.g., linear and circular dichroism). These methods are known for their sensitivity in detecting molecular anisotropy. Differential polarization imaging combines the most useful features of these methods with the ability to resolve spatially the molecular anisotropy at a microscopic level.

The results presented in this paper are this laboratory's first efforts in the development of differential polarization microscopy. We are currently concentrating on the development of a theory to establish the optical sectioning applications of this technique. These efforts are being carried out in parallel with the development of the instrumentation. By combining the theory and experimental development, we hope to contribute to a better understanding of the overall potential of this technique.

The authors thank Dr. William Mickols for his advise in the sample preparations.

This work was supported in part by a grant from the National Institutes of Health GM-32543, GRS-3-506, National Science Foundation DMB-8609654, DMB-8501824, a Searle Scholarship, and an Alfred P. Sloan Fellowship. Additional funding was provided by the Center for High Technology and Materials, UNM. C. Bustamante is a 1984 Searle Scholar and 1985 Alfred P. Sloan Fellow.

Received for publication 14 April 1987 and in final form 7 August 1987.

REFERENCES

1. Mickols, W., M. F. Maestre, I. Tinoco, Jr., and S. H. Embury. 1985. Visualization of oriented hemoglobin in individual erythrocytes by differential extinction of polarized light. *Proc. Natl. Acad. Sci. USA.* 82:6527–6531.
2. Mickols, W., I. Tinoco, Jr., M. F. Maestre, and C. Bustamante. 1985. Imaging differential polarization microscope with electronic readout. *Rev. Sci. Instrum.* 56:2228–2236.
3. Mickols, W., C. Bustamante, M. F. Maestre, I. Tinoco, Jr., and S. H. Embury. 1985. Differential polarization microscopy. *Biotechnology.* 3:711–714.
4. Allison, A. C. 1956. Properties of sickle-cell haemoglobin. *Biochem. J.* 65:212–219.
5. Hofrichter, J., D. G. Hendricker, and W. A. Eaton. 1973. Structure of hemoglobin S fibers: optical determination of the molecular orientation in sickled erythrocytes. *Proc. Natl. Acad. Sci. USA.* 70:3604–3608.
6. White, J. M. 1974. Ultrastructural features of erythrocyte and hemoglobin sickling. *Arch. Int. Med.* 133:545–562.
7. Finch, J. T., M. F. Perutz, and J. F. Bertles. 1973. Structure of sickled erythrocytes and of sickle cell hemoglobin fibers. *Proc. Natl. Acad. Sci. USA.* 70:718–772.
8. Dykes, G., R. H. Crepeau, and S. J. Edelstein. 1978. Three-dimensional reconstruction of the fibers of sickle-cell haemoglobin. *Nature (Lond.).* 272:506–510.
9. Perutz, M. F., and J. M. Mitchison. 1950. State of hemoglobin in sickle-cell anemia. *Nature (Lond.).* 166:677–682.
10. Ross, P. D., J. Hofrichter, and W. A. Eaton. 1975. Calorimetric and optical characterization of sickle cell hemoglobin gelation. *J. Mol. Biol.* 96:239–256.
11. Mizukami, H., D. E. Bartnicki, S. Burke, G. J. Brewer, and I. F. Mizukami. 1986. The effect of erythrocyte membrane on the birefringence formation of sickle cell hemoglobin. *Am. J. Hematol.* 21:233–241.
12. Peetermans, J., I. Nishio, S. T. Ohnishi, and T. Tanaka. 1986. Light-scattering study of depolymerization kinetics of sickle hemoglobin polymers inside single erythrocytes. *Proc. Natl. Acad. Sci. USA.* 83:352–356.
13. Bertles, J. F., and J. Dobler. 1969. Reversible and irreversible sickling: a distinction by electron microscopy. *Blood.* 33:884–898.
14. Madgoff-Fairchild, B., and L. S. Rosen. 1986. Plausible models of the sickle hemoglobin fiber based on x-ray diffraction data. *Biophys. J.* 49:67–69.
15. Shibata, K., G. L. Cottam, and M. R. Waterman. 1980. Acceleration of the rate of deoxyhemoglobin S polymerization by the erythrocyte membrane. *FEBS (Fed. Eur. Biochem. Soc.) Lett.* 110:107–110.
16. Goldberg, M. A., A. T. Lalos, and H. F. Bunn. 1981. The effect of membrane preparations on the polymerization of sickle hemoglobin. *J. Biochem.* 256:193–197.
17. Eaton, W. A., L. K. Hanson, P. J. Stephens, J. C. Sutherland, and J. Dunn. 1978. Optical spectra of oxy- and deoxyhemoglobin. *J. Am. Chem. Soc.* 100:4991–5003.
18. Churg, A. K., and M. W. Makinen. 1978. The electronic structure and coordination geometry of the oxyheme complex in myoglobin. *J. Chem. Phys.* 68:1913–1925.
19. Scherman, I. J. 1940. The sickling phenomenon with special reference to the differentiation of sickle cell anemia from the sickle cell trait. *Bull. Johns Hopkins Hosp.* 67:309.